APPENDIX A

NUMERICAL BASIS OF PROGRAM MFREK

There is no way to obtain analytical solution for the hydrodynamic models described in chapter 2 unless a lot of simplizations are applied to the models and its applications are very limited. With high speed supercomputer, a very accurately numerical solution could be obtained. In this study, a program MFREK, based on the hydrodynamic models, is developed to obtain numerical solution for multiphase flow systems, using supercomputer. Appendix A describes the numerical scheme while appendix B describes the organization of the program and appendix C lists the source Fortran code and a sample input data of the program.

A.1 The Governing Equations

We will consider a multiphase system consisting of several particulate phases and a continuous phase. In the following equations, gas is treated as continuous phase, but liquid could be treated as continuous phase too in some particular situations such as liquid-solid system. The particulate phases could be one or more disperse phases, for instance, liquid and catalyst in gas-liquid-solid system of chapter 4 and 5, coal and pyrite in a gas-solid-solid system of chapter 6.

A.1.1 Continuity Equations

Gas Phase:

$$\frac{\partial}{\partial t}(\varepsilon_g \rho_g)+\nabla\cdot(\varepsilon_g \rho_g \mathbf{v}_g)=\dot{m}_g$$

Liquid and Solid phases: ($k=\ell,s$)

$$\frac{\partial}{\partial t}(\varepsilon_k \rho_k)+\nabla\cdot(\varepsilon_k \rho_k \mathbf{v}_k)=\dot{m}_k$$

$$\varepsilon_g+\varepsilon_\ell+\varepsilon_s=1$$

A.1.2 Momentum Equations

Gas Phase:

$$\frac{\partial}{\partial t}(\varepsilon_g \rho_g v_g)+\nabla\cdot(\varepsilon_g \rho_g v_g v_g)=\varepsilon_g \rho_g F_g+\sum_{m=\ell,s}\beta_{gm}(v_m-v_g)+\nabla\cdot[\tau_g]+\dot{m}_g v_g$$

Liquid and Solid Phases: ($k=\ell,s$)

$$\frac{\partial}{\partial t}(\varepsilon_k \rho_k v_k)+\nabla\cdot(\varepsilon_k \rho_k v_k v_k)=\varepsilon_k \rho_k F_k+\sum_{m=g,\ell,s}\beta_{km}(v_m-v_k)+\nabla\cdot[\tau_k]+\dot{m}_k v_k$$

A.1.3 Energy Equations

Gas Phase:

$$\frac{\partial}{\partial t}(\varepsilon_g \rho_g H_g)+\nabla\cdot(\varepsilon_g \rho_g H_g v_g)=(\frac{\partial P_g}{\partial t}+P_g \nabla\cdot v_g)+\nabla\cdot(k_g \nabla T_g)+\Phi_g+\sum_i r_{ig}\Delta H_{ig}$$
$$+\sum_{m=\ell,s}\left\{h_{vm}(T_m-T_g)+\beta_{gm}(v_m-v_g)^2-\dot{m}_m H_g\right\}$$

Liquid and Solid Phases: ($k=\ell,s$)

$$\frac{\partial}{\partial t}(\varepsilon_k \rho_k H_k)+\nabla\cdot(\varepsilon_k \rho_k H_k v_k)=h_{vk}(T_g-T_k)+\sum_{m=g,\ell,s}\beta_{km}(v_m-v_k)^2+\dot{m}_k H_g$$
$$+\nabla\cdot(k_k \nabla T_k)+\sum_i r_{ik}\Delta H_{ik}+\Phi_k$$

A.2 Constitutive Equations

A.2.1 Equation of State.

$$\rho_g=\frac{\overline{M}_g P_g}{zRT_g}$$

A.2.2 Drag Coefficients

$$\beta_{gk}=\beta_{kg}=150\frac{(1-\varepsilon_g)\varepsilon_k \mu_g}{(\varepsilon_g d_k \psi_k)^2}+1.75\frac{\rho_g \varepsilon_k |v_g-v_k|}{\varepsilon_g d_k \psi_k} \qquad \varepsilon_g>0.8$$

$$\beta_{gk}=\beta_{kg}=\frac{3}{4}C_D\frac{\rho_g\varepsilon_k|v_g-v_k|}{d_k\psi_k}\varepsilon_g^{-2.65} \qquad \varepsilon_g<0.8$$

where $$C_D=\frac{24}{Re_k}(1+0.15Re_k^{0.687})$$

$$Re_k=\frac{\rho_g\varepsilon_g|v_g-v_k|d_k\psi_k}{\mu_g} \qquad Re_k=1000 \quad \text{if} \quad Re_k>1000$$

$$\beta_{\ell s}=\beta_{s\ell}=\frac{3}{2}(1+e)\frac{\rho_s\rho_\ell\varepsilon_s\varepsilon_s|v_\ell-v_s|}{\rho_s d_s^3+\rho_\ell d_\ell^3}(d_s+d_\ell)^2$$

A.2.3 External Forces Acting on Each Phase

$$F_g=\frac{g}{\varepsilon_g}$$

$$F_k=\frac{g}{\varepsilon_g}\left(1-\frac{1}{\rho_k}\sum_{m=g,\ell,s}\varepsilon_m\rho_m\right)+q_kE \qquad k=\ell,s$$

A.2.4 Shear Stresses

$$[\tau_g]=\left\{-P_g-\frac{2}{3}\mu_g\varepsilon_g\nabla\cdot v_g\right\}[I]+\mu_g\varepsilon_g\left[\nabla v_g+(\nabla v_g)^T\right]$$

$$[\tau_k]=\left\{-P_k+\tau_{ck}+\left(\xi_k-\frac{2}{3}\mu_k\right)\nabla\cdot v_k\right\}[I]+\mu_k\left[\nabla v_k+(\nabla v_k)^T\right] \qquad k=\ell,s$$

$$\tau_{ck}=10^{10.6\varepsilon_k+5.5} \qquad k=\ell,s$$

Empirical Solids Viscosity and Stress Model (optional, a substitution to kinetic theory).

$$\mu_k=5\varepsilon_k \qquad \xi_k=0$$

$$\nabla P_k=G(\varepsilon_k)\nabla\varepsilon_k \qquad G(\varepsilon_k)=10^{8.76\varepsilon_k-0.27}$$

A.2.5 Enthalpy

$$H_g = C_{p_g}(T_g - T_g^0)$$

$$H_k = C_{p_k}(T_k - T_k^0)$$

A.2.6 Gas-Solid Heat Transfer. (Gunn's Model)

$$Nu_k = \left\{(2+5\varepsilon_k^2)(1+0.7Re_k^{0.2}Pr^{1/3}) + (\frac{2}{15}+1.2\varepsilon_k^2)Re_k^{0.7}Pr^{1/3}\right\}Sp_k$$

$$Nu_k = \frac{h_{vk}d_k}{k_g^0} \qquad Pr = \frac{C_{p_g}\mu_g}{k_g^0} \qquad Sp_k = \frac{6\varepsilon_k}{d_k}$$

A.2.7 Gas Phase Heat Transfer

$$k_g^0 = 8.65\times10^5\left(\frac{T_g}{1400}\right)^{1.786}$$

$$k_g = (1-\sqrt{1-\varepsilon_g})k_g^0$$

A.2.8 Particulate Phase Heat Transfer

$$\frac{k_k}{k_g^0} = \frac{\sqrt{\varepsilon_s}}{(1-\varepsilon_g)}\left\{\varphi\frac{k_k^*}{k_g^0} + (1-\varphi)\frac{k_k^0}{k_g^0}\right\}$$

$$\frac{k_k^0}{k_g^0} = \frac{2}{A_k}\left\{\frac{B_k\left\{(k_k^*/k_g^0)-1\right\}}{A_k^2(k_k^*/k_g^0)}\ln\frac{(k_k^*/k_g^0)}{B_k} - \frac{B_k-1}{A_k} - \frac{B_k+1}{2}\right\}$$

where

$$A_k = 1 - \frac{B_k}{(k_k^*/k_g^0)}$$

$$B_k = 1.25\left(\frac{\varepsilon_k}{\varepsilon_g}\right)^{10/9}(1+3\chi)$$

$$\chi=\sqrt{\frac{\left(\sum\varepsilon_k\rho_k\right)\left(\sum\varepsilon_k\rho_k/d_k^2\right)}{\left(\sum\varepsilon_k\rho_k/d_k\right)^2}-1} \qquad k=l,s$$

$$k_k^*=0.3289 \qquad \varphi=7.26\times10^{-3}$$

A.3 Solid Viscosity from Kinetic Theory

A.3.1 Fluctuating Energy Equation. (k=ℓ,s)

$$\frac{3}{2}\left[\frac{\partial}{\partial t}(\varepsilon_k\rho_k\Theta_k)+\nabla\cdot(\varepsilon_k\rho_k\Theta_k v_k)\right]=\nabla\cdot(\kappa_k\nabla\Theta_k)-\gamma_k-3\beta_{kg}\Theta_k+\Phi_k$$

A.3.2 Energy Production Rate

$$\Phi_k=[\tau_k]:\nabla v_k \qquad k=g,\ell,s$$

A.3.3 Conductive Coefficient of Fluctuating Energy

$$\kappa_k=\frac{2\kappa_{k_{as}}}{(1+e_k)g_{0k}}\left\{1+\frac{6}{5}(1+e_k)g_{0k}\varepsilon_k\right\}^2+2\varepsilon_k^2\rho_k d_k g_{0k}(1+e_k)\sqrt{\frac{\Theta_k}{\pi}}$$

A.3.4 Collisional Energy Dissipation

$$\gamma_k=3(1-e_k^2)\varepsilon_k^2\rho_k g_{0k}\Theta_k\left\{\frac{4\sqrt{\Theta_k}}{d_k\sqrt{\pi}}-\nabla\cdot v_k\right\}$$

A.3.5 Solids Pressure

$$P_k=\rho_k\varepsilon_k\Theta_k\{1+2(1+e_k)g_{0k}\varepsilon_k\}$$

A.3.6 Solids Bulk Viscosity

$$\xi_k=\frac{4}{3}\varepsilon_k^2\rho_k d_k g_{0k}(1+e_k)\sqrt{\frac{\Theta_k}{\pi}}$$

A.3.7 Solids Shear Viscosity

$$\mu_k=\frac{2\mu_{k_{as}}}{(1+e_k)g_{0k}}\left\{1+\frac{4}{5}(1+e_k)g_{0k}\varepsilon_s\right\}^2+\frac{4}{5}\varepsilon_k^2\rho_k d_k g_{0k}(1+e_k)\sqrt{\frac{\Theta_k}{\pi}}$$

Where

$$g_{0k}=\left\{1-\left(\frac{\varepsilon_k}{\varepsilon_{k_{max}}}\right)^{1/3}\right\}^{-1} \qquad \mu_{k_{dil}}=\frac{5}{96}\rho_k d_k\sqrt{\pi\Theta_k} \qquad \kappa_{k_{dil}}=\frac{75}{384}\rho_k d_k\sqrt{\pi\Theta_k}$$

A.4 Reaction and Mass Transfer

A.4.1 General Reactions

$$\sum_j^N \alpha_{ik}^j S^j=0 \qquad i=1,2,\cdots,M_k \qquad k=g,\ell,s$$

$$r_{ik}=f_{ik}(P_k,T_k,\varepsilon_k,y_k^1,y_k^2,\cdots,y_k^N,\cdots) \qquad i=1,2,\cdots,M_k \quad k=g,\ell,s$$

A.4.2 Mass Transfer Between Phases

$$R_k^j=f_k^j(P_k,T_k,a_k,y_k^1,y_k^2,\cdots,y_k^N,P_g,T_g,y_g^1,y_g^2,\cdots,y_g^N,\cdots) \qquad k=\ell,s$$

A.5 Species Balances (j=1, 2, ..., N)

A.5.1 Gas Phase:

$$\frac{\partial}{\partial t}(\varepsilon_g\rho_g y_g^j)+\nabla\cdot(\varepsilon_g\rho_g y_g^j v_g)=\sum_{i=1}^{M_g}\alpha_{ig}^j M^j r_{ig}-\sum_{k=\ell,s}M^j R_k^j$$

A.5.2 Liquid and Solid Phases: (k=ℓ,s)

$$\frac{\partial}{\partial t}(\varepsilon_k\rho_k y_k^j)+\nabla\cdot(\varepsilon_k\rho_k y_k^j v_k)=\sum_{i=1}^{M_k}\alpha_{ik}^j M^j r_{ik}+M^j R_k^j$$

$$\sum_j^N y_k^j=1 \qquad k=g,\ell,s$$

A.5.3 Phase Changes: (k=ℓ,s) $\qquad \dot{m}_k=\sum_j^N M^j R_k^j \qquad \dot{m}_g=-\sum_{k=\ell,s}\dot{m}_k$

A.6 The Finite Difference Equations

The computations are carried out using a two-dimensional Eulerian mesh of non-uniform size finite-difference computational cells. These cells are rectangles with

dimensions dx_i (or dr_i) and dy_j (or dz_j). A typical mesh with cell flag (define the type of the cell) and computational cell (i, j) are shown in Figure A.1. The indexes i and j that label cell (i, j) count cell centers in the x-direction and y-direction, respectively, and assume only positive integer values. The scalar variables (ε_k, ρ_k, P_k, T_k, H_k, y_k^j, $\cdots$) are located at the cell center and the vector variables (v_k, $[\tau_k]$, $\cdots$) at the cell boundaries.

The finite-difference approximations to the hydrodynamic equations form a system of nonlinear algebraic equations relating quantities at time t=(n+1)dt, where n is zero or a positive integer and dt is the time increment by which these quantities advance each computational cycle.

A.6.1 Averaging Process. Quantities in the finite difference equations required at spatial locations other than where they are defined are obtained by weighted averaging.

(a) Cell Centered Quantities. The cell centered properties Ψ are defined at the cell center of (i, j). At other locations averaging is used as follows,

$$\Psi_{i+\frac{1}{2},j}=\frac{1}{2\delta r_{i+\frac{1}{2}}}(\delta r_{i+1}\Psi_{i,j}+\delta r_i\Psi_{i+1,j})$$

$$\Psi_{i,j+\frac{1}{2}}=\frac{1}{2\delta z_{j+\frac{1}{2}}}(\delta z_{j+1}\Psi_{i,j}+\delta z_j\Psi_{i,j+1})$$

$$\Psi_{i+\frac{1}{2},j+\frac{1}{2}}=\frac{1}{4\delta r_{i+\frac{1}{2}}\delta z_{j+\frac{1}{2}}}(\delta r_{i+1}\delta z_{j+1}\Psi_{i,j}+\delta r_i\delta z_{j+1}\Psi_{i+1,j}$$
$$+\delta r_{i+1}\delta z_j\Psi_{i,j+1}+\delta r_i\delta z_j\Psi_{i+1,j+1})$$

(b) Boundary Centered Quantities. The boundary centered quantity in x-direction is u which defined at (i, j+1/2). The averaging is as follows,

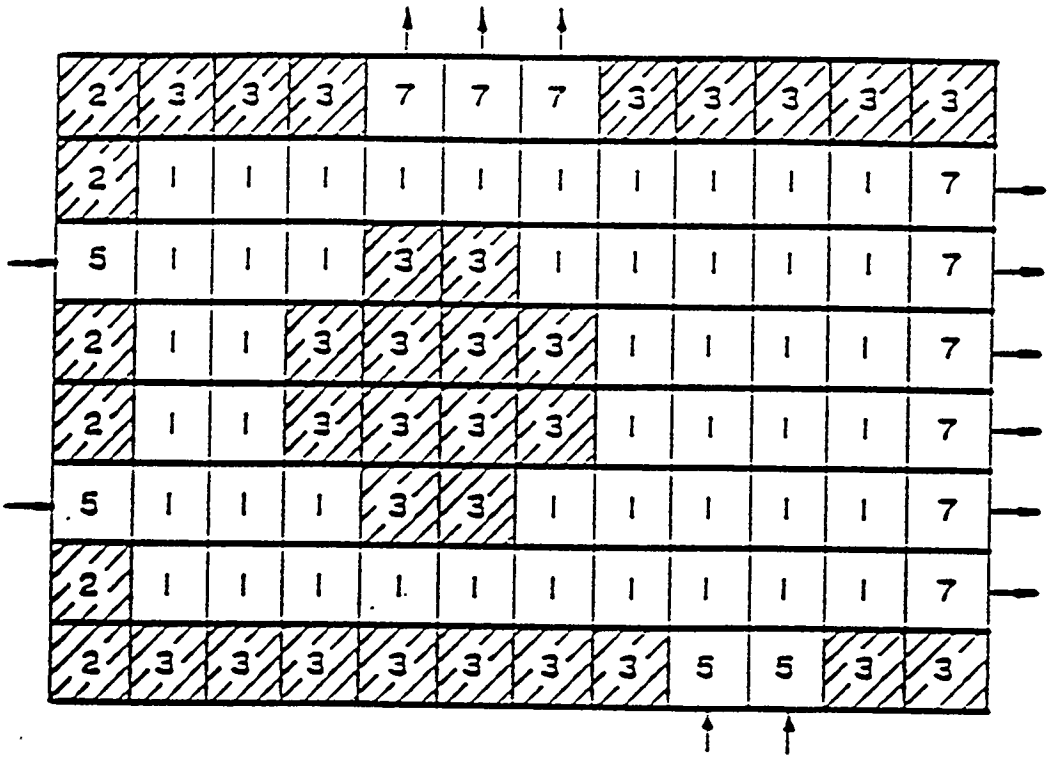

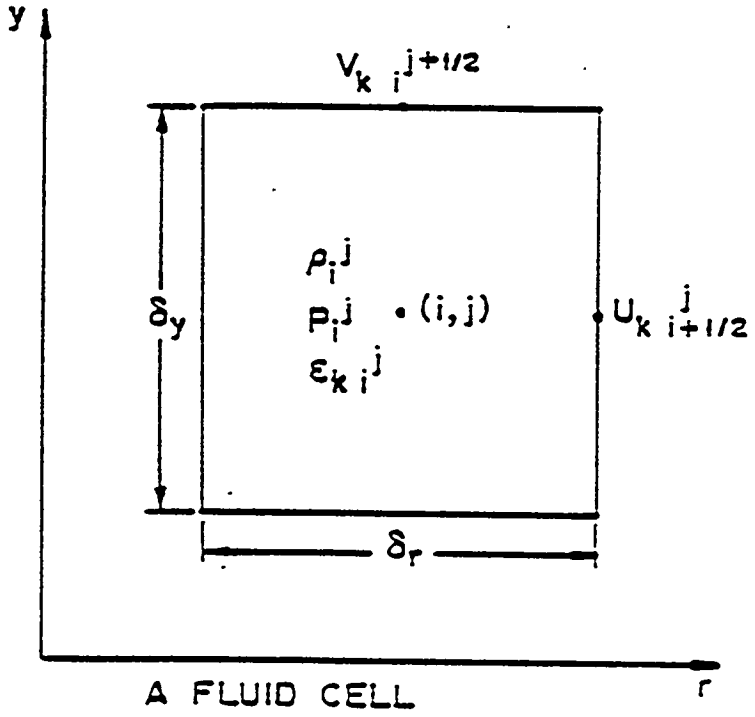

Figure A.1 The Computational Mesh

$$u_{i,j}=\frac{1}{2}(u_{i+\frac{1}{2},j}+u_{i+\frac{1}{2},j+1})$$

$$u_{i+\frac{1}{2},j+\frac{1}{2}}=\frac{1}{2\delta z_{j+\frac{1}{2}}}(\delta z_{j+1}u_{i+\frac{1}{2},j}+\delta z_j u_{i+\frac{1}{2},j+1})$$

$$u_{i,j+\frac{1}{2}}=\frac{1}{4\delta z_{j+\frac{1}{2}}}(\delta z_{j+1}(u_{i-\frac{1}{2},j}+u_{i+\frac{1}{2},j})+\delta z_j(u_{i-\frac{1}{2},j+1}+u_{i+\frac{1}{2},j+1}))$$

The boundary centered quantity in y-direction is v which defined at (i+1/2, j). The averaging is as follows,

$$v_{i,j}=\frac{1}{2}(v_{i+\frac{1}{2},j}+v_{i+\frac{1}{2},j+1})$$

$$v_{i+\frac{1}{2},j+\frac{1}{2}}=\frac{1}{2\delta r_{i+\frac{1}{2}}}(\delta r_{i+1}u_{i,j+\frac{1}{2}}+\delta r_i v_{i+1,j+\frac{1}{2}})$$

$$v_{i+\frac{1}{2},j}=\frac{1}{4\delta r_{i+\frac{1}{2}}}(\delta r_{i+1}(v_{i,j-\frac{1}{2}}+v_{i,j+\frac{1}{2}})+\delta r_i(v_{i+1,j-\frac{1}{2}}+v_{i+1,j+\frac{1}{2}}))$$

A.6.2 Continuity Equations. The continuity equations are differenced fully implicitly as follows, ($k=g,\ell,s$)

$$(\rho_k\varepsilon_k)_{i,j}^{n+1}=(\rho_k\varepsilon_k)_{i,j}^{n}-\frac{\delta t}{\delta r_i}\langle(\rho_k\varepsilon_k)u_k\rangle_{i,j}^{n+1}-\frac{\delta t}{\delta z_j}\langle(\rho_k\varepsilon_k)v_k\rangle_{i,j}^{n+1}+\delta t\cdot(\dot{m}_k)_{i,j}^{n}$$

The donor cell differencing aids computational stability without the introduction of explicit artificial viscosity.

A.6.3 Momentum Equations. The momentum equations are differenced over a staggered mesh (Figure A.2) using a scheme in which the convective terms are treated explicitly and all other terms are treated implicitly. the difference equations are,

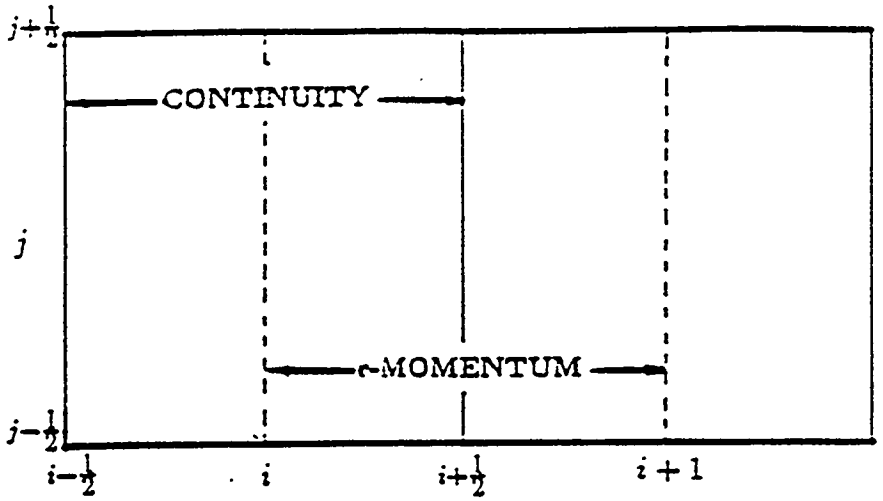

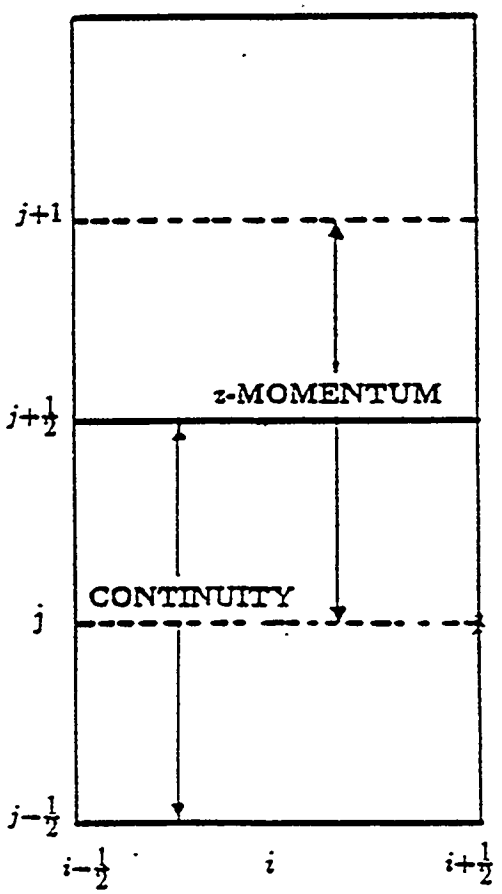

Figure A.2 The Staggered Computational Mesh for Momentum equations

$$(\rho_k\varepsilon_k u_k)^{n+1}_{i+\frac{1}{2},j}=(\overline{\rho_k\varepsilon_k u_k})_{i+\frac{1}{2},j}-\frac{\delta t}{\delta r_{i+\frac{1}{2}}}\left((P_k)^{n+1}_{i+1,j}-(P_k)^{n+1}_{i,j}\right)$$

$$-(w_k)^{n+1}_{i+\frac{1}{2},j}g_r\delta t+\delta t\sum_{m=g,\ell,s}(\beta_{mk})^n_{i+\frac{1}{2},j}\left((u_m)^{n+1}_{i+\frac{1}{2},j}-(u_k)^{n+1}_{i+\frac{1}{2},j}\right)$$

$$+\frac{\delta t}{\delta r_{i+\frac{1}{2}}}\left((\tau_{ck})^{n+1}_{i+1,j}-(\tau_{ck})^{n+1}_{i,j}\right)+\delta t\cdot(\dot{m}_k)^n_{i,j}(u_k)^{n+1}_{i+\frac{1}{2},j}$$

$$(\rho_k\varepsilon_k v_k)^{n+1}_{i,j+\frac{1}{2}}=(\overline{\rho_k\varepsilon_k v_k})_{i,j+\frac{1}{2}}-\frac{\delta t}{\delta z_{j+\frac{1}{2}}}\left((P_k)^{n+1}_{i,j+1}-(P_k)^{n+1}_{i,j}\right)$$

$$-(w_k)^{n+1}_{i,j+\frac{1}{2}}g_z\delta t+\delta t\sum_{m=\ell,g,s}(\beta_{mk})^n_{i,j+\frac{1}{2}}\left((v_m)^{n+1}_{i,j+\frac{1}{2}}-(v_k)^{n+1}_{i,j+\frac{1}{2}}\right)$$

$$+\frac{\delta t}{\delta r_{j+\frac{1}{2}}}\left((\tau_{ck})^{n+1}_{i,j+1}-(\tau_{ck})^{n+1}_{i,j}\right)+\delta t\cdot(\dot{m}_k)^n_{i,j}(v_k)^{n+1}_{i,j+\frac{1}{2}}$$

where for gas phase $w_g=\rho_g$ **and** $\tau_{cg}=0$, and for particulate phases

$$w_k=\frac{\varepsilon_k}{\varepsilon_g}(\rho_k-\sum_{m=g,\ell,s}\varepsilon_m\rho_m)\qquad k=\ell,s.$$

All the explicit terms are lumped into the "tilde" quantities as shown below,

$$(\overline{\rho_k\varepsilon_k u_k})_{i+\frac{1}{2},j}=(\rho_k\varepsilon_k u_k)^n_{i+\frac{1}{2},j}-\frac{\delta t}{\delta r_{i+\frac{1}{2}}}\langle(\rho_k\varepsilon_k u_k)u_k\rangle^n_{i+\frac{1}{2},j}-\frac{\delta t}{\delta z_j}\langle(\rho_k\varepsilon_k u_k)v_k\rangle^n_{i+\frac{1}{2},j}$$

$$+\frac{\delta t}{\delta r_{i+\frac{1}{2}}}\left((\tau_{krr})^n_{i+1,j}-(\tau_{krr})^n_{i,j}\right)+\frac{\delta t}{\delta z_j}\left((\tau_{krz})^n_{i+\frac{1}{2},j+\frac{1}{2}}-(\tau_{krz})^n_{i+\frac{1}{2},j-\frac{1}{2}}\right)$$

$$(\overline{\rho_k\varepsilon_k v_k})_{i,j+\frac{1}{2}}=(\rho_k\varepsilon_k v_k)^n_{i,j+\frac{1}{2}}-\frac{\delta t}{\delta r_i}\langle(\rho_k\varepsilon_k v_k)u_k\rangle^n_{i,j+\frac{1}{2}}-\frac{\delta t}{\delta z_{j+\frac{1}{2}}}\langle(\rho_k\varepsilon_k v_k)v_k\rangle^n_{i,j+\frac{1}{2}}$$

$$+\frac{\delta t}{\delta r_i}\left((\tau_{krz})^n_{i+\frac{1}{2},j+\frac{1}{2}}-(\tau_{krz})^n_{i-\frac{1}{2},j+\frac{1}{2}}\right)+\frac{\delta t}{\delta z_{j+\frac{1}{2}}}\left((\tau_{kzz})^n_{i+,j+1}-(\tau_{kzz})^n_{i,j}\right)$$

A.6.4 Energy Equations

(a) Gas Phase.

$$(\rho_g\varepsilon_g H_g)^{n+1}_{i,j}=(\rho_g\varepsilon_g H_g)^{n}_{i,j}+\overline{(\rho_g\varepsilon_g H_g)_{i,j}}+\delta t\sum_{k=\ell,s}(h_{vk})^{n}_{i,j}(T_k-T_g)^{n+1}_{i,j}$$

$$+\delta t\sum_{k=\ell,s}(\beta_{kg})^{n}_{i,j}\left\{\left((u_k)^{n}_{i,j}-(u_g)^{n}_{i,j}\right)^2+\left((v_k)^{n}_{i,j}-(v_g)^{n}_{i,j}\right)^2\right\}+\delta t\cdot(\dot{Q}_{rg}+\dot{Q}_{fg})^{n}_{i,j}$$

(b) Solid Phases.

$$(\rho_k\varepsilon_k H_k)^{n+1}_{i,j}=(\rho_k\varepsilon_k H_k)^{n}_{i,j}+\overline{(\rho_k\varepsilon_k H_k)_{i,j}}+\delta t(h_{vk})^{n}_{i,j}(T_g-T_k)^{n+1}_{i,j}+\delta t\cdot(\dot{Q}_{rk}+\dot{Q}_{fk})^{n}_{i,j}$$

(c) "Tilde" quantities are given by,

$$\overline{(\rho_g\varepsilon_g H_g)_{i,j}}=\frac{\delta t}{\delta r_i}\left\langle(\rho_g\varepsilon_g)^{n+1}\overline{H}_g(u_g)^{n+1}\right\rangle_{i,j}\frac{\delta t}{\delta z_j}\left\langle(\rho_g\varepsilon_g)^{n+1}\overline{H}_g(u_g)^{n+1}\right\rangle_{i,j}$$

$$+\left((P_g)^{n+1}_{i,j}-(P_g)^{n}_{i,j}\right)+\frac{\delta t}{\delta r_i}(u_g)^{n+1}_{i,j}\left((P_g)^{n+1}_{i+\frac{1}{2},j}-(P_g)^{n+1}_{i-\frac{1}{2},j}\right)$$

$$\frac{\delta t}{\delta z_j}(v_g)^{n+1}_{i,j}\left((P_g)^{n+1}_{i,j+\frac{1}{2}}-(P_g)^{n+1}_{i,j-\frac{1}{2}}\right)$$

$$\overline{(\varepsilon_k\rho_k H_k)_{i,j}}=\frac{\delta t}{\delta r_i}\left\langle(\varepsilon_k\rho_k)^{n+1}\overline{H}_k(u_k)^{n+1}\right\rangle_{i,j}\frac{\delta t}{\delta z_j}\left\langle(\varepsilon_k\rho_k)^{n+1}\overline{H}_k(v_k)^{n+1}\right\rangle_{i,j}$$

$$+\frac{\delta t}{\delta r_i}\left((K_k)^{n}_{i+\frac{1}{2},j}\frac{(\overline{T}_k)_{i+1,j}-(\overline{T}_k)_{i,j}}{\delta r_{i+\frac{1}{2}}}-(K_k)^{n}_{i-\frac{1}{2},j}\frac{(\overline{T}_k)_{i,j}-(\overline{T}_k)_{i-1,j}}{\delta r_{i-\frac{1}{2}}}\right)$$

$$+\frac{\delta t}{\delta z_j}\left((K_k)^{n}_{i,j+\frac{1}{2}}\frac{(\overline{T}_k)_{i,j+1}-(\overline{T}_k)_{i,j}}{\delta z_{i+\frac{1}{2}}}-(K_k)^{n}_{i,j-\frac{1}{2}}\frac{(\overline{T}_k)_{i,j}-(\overline{T}_k)_{i,j-1}}{\delta z_{i-\frac{1}{2}}}\right)+\delta t(\Phi_k)^{n}_{i,j}$$

$$(\Phi_k)^{n}_{i,j}=(\tau_{krr})^{n}_{i,j}\frac{(u_k)^{n+1}_{i+\frac{1}{2},j}-(u_k)^{n+1}_{i-\frac{1}{2},j}}{\delta r_i}+(\tau_{kzz})^{n}_{i,j}\frac{(v_k)^{n+1}_{i,j+\frac{1}{2}}-(v_k)^{n+1}_{i,j-\frac{1}{2}}}{\delta z_j}+\frac{\left((\tau_{krz})^{n}_{i,j}\right)^2}{2(\mu_k)^{n}_{i,j}}$$

$$(\dot{Q}_{rg})^n_{i,j}=\sum_{ix=1}^{ixn}(r_{ixg})^n_{i,j}(\Delta H_{ixg})^n_{i,j}-\sum_{m=\ell,s}(\dot{m}_m)^n_{i,j}(H_g)^n_{i,j}$$

$$(\dot{Q}_{fg})^n_{i,j}=\begin{cases}0 & \text{if cell (i,j) has no contact with a heat boundary or block}\\ (C_{fx}\varepsilon_g)^n_{i,j} & \text{if cell (i,j) contacts a heat boundary or block with constant heat flux}\\ \left(K_B\varepsilon_g(T_B-T_g)\right)^n_{i,j} & \text{if cell (i,j) contacts a heat boundary or block with constant temperature}\end{cases}$$

$$(\dot{Q}_{rk})^n_{i,j}=(\dot{m}_k)^n_{i,j}(H_g)^n_{i,j}+\sum_{ix=1}^{ixn}(r_{ixk})^n_{i,j}(\Delta H_{ixk})^n_{i,j}$$

$$(\dot{Q}_{fk})^n_{i,j}=\begin{cases}0 & \text{if cell (i,j) has no contact with a heat boundary or block}\\ (C_f\varepsilon_k)^n_{i,j} & \text{if cell (i,j) contacts a heat boundary or block with constant heat flux}\\ \left(K_B\varepsilon_k(T_B-T_k)\right)^n_{i,j} & \text{if cell (i,j) contacts a heat boundary or block with constant temperature}\end{cases}$$

A.6.5 Species Balance. (k=g,ℓ,s), j=the j−th species.

$$(\rho_k\varepsilon_k y^j_k)^{n+1}_{i,j}=(\rho_k\varepsilon_k y^j_k)^n_{i,j}-\frac{\delta t}{\delta r_i}\left\langle(\rho_k\varepsilon_k y^j_k)u_k\right\rangle^{n+1}_{i,j}-\frac{\delta t}{\delta z_j}\left\langle(\rho_k\varepsilon_k y^j_k)v_k\right\rangle^{n+1}_{i,j}+\delta t\cdot(\dot{m}_k)^n_{i,j}$$

As mentioned before, the flux quantities denoted by $\langle \psi u_k \rangle$ and $\langle \psi v_k \rangle$ are calculated using donor-cell differencing, where ψ refers to quantities:

$$\varepsilon_k\rho_k,\ \varepsilon_k\rho_k u_k,\ \varepsilon_k\rho_k v_k,\ \varepsilon_k\rho_k \overline{\overline{H}}_k,\ \varepsilon_k\rho_k y_k^j u_k,\ \varepsilon_k\rho_k y_k^j v_k \qquad k=g,\ell,s$$

The angular brackets represent donor cell differenced quantities as shown below,

$$\langle \Psi u_k \rangle_{m,p} = (u_k)_{m+\frac{1}{2},p} \begin{cases} (\Psi)_{m,p} & \text{if } (u_k)_{m+\frac{1}{2},p} \geq 0 \\ (\Psi)_{m+1,p} & \text{if } (u_k)_{m+\frac{1}{2},p} < 0 \end{cases} - (u_k)_{m-\frac{1}{2},p} \begin{cases} (\Psi)_{m-1,p} & \text{if } (u_k)_{m-\frac{1}{2},p} \geq 0 \\ (\Psi)_{m,p} & \text{if } (u_k)_{m-\frac{1}{2},p} < 0 \end{cases}$$

$$\langle \Psi v_k \rangle_{m,p} = (v_k)_{m,p+\frac{1}{2}} \begin{cases} (\Psi)_{m,p} & \text{if } (v_k)_{m,p+\frac{1}{2}} \geq 0 \\ (\Psi)_{m,p+1} & \text{if } (v_k)_{m,p+\frac{1}{2}} < 0 \end{cases} - (v_k)_{m,p-\frac{1}{2}} \begin{cases} (\Psi)_{m,p-1} & \text{if } (v_k)_{m,p-\frac{1}{2}} \geq 0 \\ (\Psi)_{m,p} & \text{if } (v_k)_{m,p-\frac{1}{2}} < 0 \end{cases}$$

The viscous stress components are calculated with standard centered differencing, i.e.,

$$(\nabla \cdot V_k)_{i,j} = \frac{(u_k)_{i+\frac{1}{2},j} - (u_k)_{i-\frac{1}{2},j}}{\delta r_i} + \frac{(v_k)_{i,j+\frac{1}{2}} - (v_k)_{i,j-\frac{1}{2}}}{\delta z_j}$$

$$(\tau_{krr})_{i,j}=2(\mu_k)_{i,j}\left(\frac{(u_k)_{i+\frac{1}{2},j}-(u_k)_{i-\frac{1}{2},j}}{\delta r_i}\right)+(\xi_k-\frac{2}{3}\mu_k)_{i,j}(\nabla\cdot V_k)_{i,j}$$

$$(\tau_{kzz})_{i,j}=2(\mu_k)_{i,j}\left(\frac{(v_k)_{i,j+\frac{1}{2}}-(v_k)_{i,j-\frac{1}{2}}}{\delta z_j}\right)+(\xi_k-\frac{2}{3}\mu_k)_{i,j}(\nabla\cdot V_k)_{i,j}$$

$$(\tau_{krz})_{i,j}=2(\mu_k)_{i,j}\left(\frac{(u_k)_{i,j+1}-(u_k)_{i,j-1}}{\delta z_{j-\frac{1}{2}}+\delta z_{j+\frac{1}{2}}}+\frac{(v_k)_{i+1,j}-(v_k)_{i-1,j}}{\delta r_{i-\frac{1}{2}}+\delta r_{i+\frac{1}{2}}}\right)$$

$$(\tau_{krz})_{i+\frac{1}{2},j+\frac{1}{2}}=2(\mu_k)_{i+\frac{1}{2},j+\frac{1}{2}}\left(\frac{(u_k)_{i+\frac{1}{2},j+1}-(u_k)_{i+\frac{1}{2},j}}{\delta z_{j+\frac{1}{2}}}+\frac{(v_k)_{i+1,j+\frac{1}{2}}-(v_k)_{i,j-\frac{1}{2}}}{\delta r_{i+\frac{1}{2}}}\right)$$

A.6.6. Fluctuating Energy Equation

$$\frac{2}{3}(\varepsilon_k\rho_k\Theta_k)_{i,j}^{n+1}=\frac{2}{3}(\varepsilon_k\rho_k\Theta_k)_{i,j}^{n}+(\overline{\varepsilon_k\rho_k\Theta_k})_{i,j}-\delta t(P_k)_{i,j}^{n+1}(\nabla\cdot V_k)_{i,j}^{n+1}$$
$$+\delta t(\Phi_k)_{i,j}^{n+1}-\delta t(\gamma_k)_{i,j}^{n+1}-3\delta t(\beta_{gk})_{i,j}^{n}(\Theta_k)_{i,j}^{n+1}$$

$$(\overline{\varepsilon_k\rho_k\Theta_k})_{i,j}=\frac{2\,\delta t}{3\delta r_i}\left\langle(\varepsilon_k\rho_k)^{n+1}(\Theta_k)^{n}(u_k)^{n+1}\right\rangle_{i,j}$$
$$\frac{2\,\delta t}{3\delta z_j}\left\langle(\varepsilon_k\rho_k)^{n+1}(\Theta_k)^{n}(v_k)^{n+1}\right\rangle_{i,j}$$
$$+\frac{\delta t}{\delta r_i}\left((\kappa_k)_{i+\frac{1}{2},j}^{n}\frac{(\Theta_k)_{i+1,j}-(\Theta_k)_{i,j}}{\delta r_{i+\frac{1}{2}}}-(\kappa_k)_{i-\frac{1}{2},j}^{n}\frac{(\Theta_k)_{i,j}-(\Theta_k)_{i-1,j}}{\delta r_{i-\frac{1}{2}}}\right)$$
$$+\frac{\delta t}{\delta z_j}\left((\kappa_k)_{i,j+\frac{1}{2}}^{n}\frac{(\Theta_k)_{i,j+1}-(\Theta_k)_{i,j}}{\delta z_{i+\frac{1}{2}}}-(\kappa_k)_{i,j-\frac{1}{2}}^{n}\frac{(\Theta_k)_{i,j}-(\Theta_k)_{i,j-1}}{\delta z_{i-\frac{1}{2}}}\right)$$

A.7 Solution Technique for Finite -Difference Equations

An iterative technique is used to solve the difference equations given in the previous section. The solution technique for finite -difference equations may be applied to any multiple particulate phases, not limited liquid and solid.

A.7.1 Solution of the Momentum Equations. To facilitate the particular method of solution the equations are recast in the following form. The momentum equations in x-direction could be collected together in a matrix form.

$$(A)_{i+\frac{1}{2},j}(U)^n_{i+\frac{1}{2},j}=(B_u)_{i+\frac{1}{2},j}$$

$$A=\begin{pmatrix} A_{gg} & A_{g1} & A_{g2} & \cdots & A_{gN} \\ A_{1g} & A_{11} & A_{12} & \cdots & A_{1N} \\ \vdots & \vdots & \vdots & \ddots & \vdots \\ A_{Ng} & A_{N1} & A_{N2} & \cdots & A_{NN} \end{pmatrix}$$

where

$$A_{kk}=(\varepsilon_k\rho_k)^{n+1}+\delta t\sum_{\substack{\ell=g,1\\ \ell\neq k}}^{N}(\beta_{\ell k})^n-\delta t(\dot{m}_k)^n \quad k=g,1,2,\cdots,N$$

$$A_{km}=A_{mk}=-\delta t(\beta_{mk})^n \quad k,m=g,1,2,\cdots,N \quad m\neq k$$

$$A_{i+\frac{1}{2},j}\cdot\begin{pmatrix} u_g \\ u_1 \\ \vdots \\ u_N \end{pmatrix}=\begin{pmatrix} (\overline{\varepsilon_g\rho_g u_g})-\dfrac{\delta t}{\delta r_{i+\frac{1}{2}}}\left((P_g+\tau_{cg})^{n+1}_{i+1,j}-(P_g+\tau_{cg})^{n+1}_{i,j}\right)-(w_g)g_r\delta t \\ (\overline{\varepsilon_1\rho_1 u_1})-\dfrac{\delta t}{\delta r_{i+\frac{1}{2}}}\left((P_1+\tau_{c1})^{n+1}_{i+1,j}-(P_1+\tau_{c1})^{n+1}_{i,j}\right)-(w_1)g_r\delta t \\ \vdots \\ (\overline{\varepsilon_N\rho_N u_N})-\dfrac{\delta t}{\delta r_{i+\frac{1}{2}}}\left((P_N+\tau_{cN})^{n+1}_{i+1,j}-(P_N+\tau_{cN})^{n+1}_{i,j}\right)-(w_N)g_r\delta t \end{pmatrix}$$

where for gas phase $w_g=\rho_g$ **and** $\tau_{cg}=0$, and for particulate phases

$$w_k=\frac{\varepsilon_k}{\varepsilon_g}(\rho_k-\sum_{m=g,1}^{N}\varepsilon_m\rho_m) \qquad k=1,2,\cdots,N.$$

and similarly, momentum equation in y-direction can be written as,

$$(A)_{i,j+\frac{1}{2}}(V)^n_{i,j+\frac{1}{2}}=(B_v)_{i,j+\frac{1}{2}}$$

$$A_{i,j+\frac{1}{2}}\cdot\begin{pmatrix}v_g\\v_1\\\vdots\\v_N\end{pmatrix}=\begin{pmatrix}\overline{(\varepsilon_g\rho_g v_g)}-\frac{\delta t}{\delta z_{j+\frac{1}{2}}}\left((P_g+\tau_{cg})^{n+1}_{i,j+1}-(P_g+\tau_{cg})^{n+1}_{i,j}\right)-(w_g)g_z\delta t\\\overline{(\varepsilon_1\rho_1 v_1)}-\frac{\delta t}{\delta z_{j+\frac{1}{2}}}\left((P_1+\tau_{c1})^{n+1}_{i,j+1}-(P_1+\tau_{c1})^{n+1}_{i,j}\right)-(w_k)g_z\delta t\\\vdots\\\overline{(\varepsilon_N\rho_N v_N)}-\frac{\delta t}{\delta z_{j+\frac{1}{2}}}\left((P_N+\tau_{cN})^{n+1}_{i,j+1}-(P_N+\tau_{cN})^{n+1}_{i,j}\right)-(w_N)g_z\delta t\end{pmatrix}$$

A.7.2 Convergence on Fluid Continuity Equation. The solution process is carried out in three major steps. First of all, the continuity equations, the momentum equations, and a part of energy equation are solved simultaneously to establish the pressure and the velocity fields. In this step only the interface heat transfer part of the energy equation is considered. Secondly, the remaining parts of the energy equations are solved to establish the temperature profiles. Finally, the compositions for each phase are solved based on the pressure and the velocity fields, volume fraction and temperature profiles obtained from the previous steps. The solution procedure of computational sweep is illustrated in Figure A.3.

The first step proceeds as follows: The calculations are started with a guessed pressure field that is either the specified initial condition or the pressure field computed in the previous time

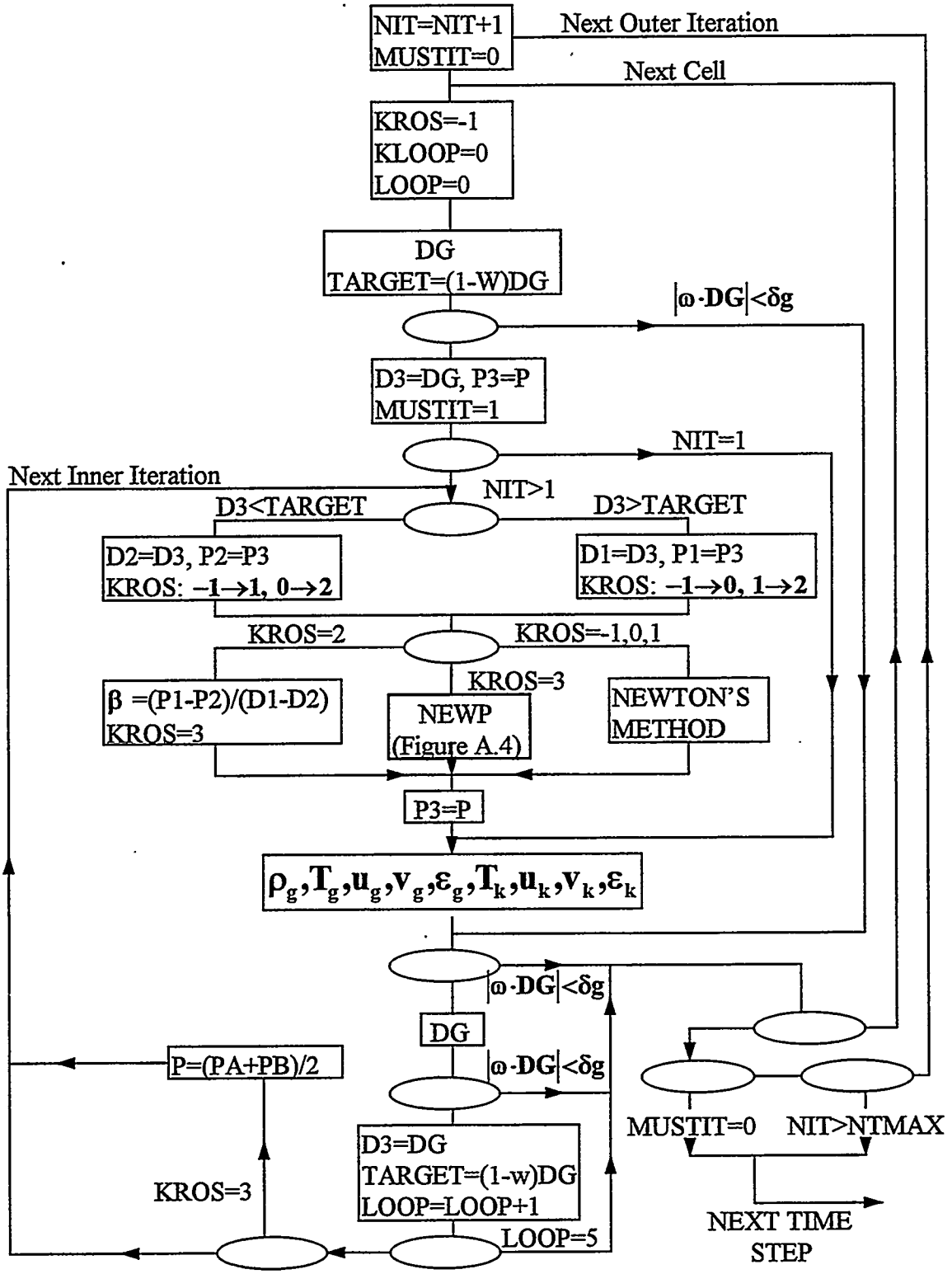

Figure A.3 The Computational Sweep

step. Using this guessed pressure field, the velocities are calculated from the matrices above. The particulate phase continuity equations are solved using the updated velocities to calculate the particulate phase volume fractions. The gas volume fraction, ε_g, is then calculated from the following equation,

$$\varepsilon_g = 1 - \sum_{k=1}^{N} \varepsilon_k$$

Using ε_g and the updated fluid velocities, the residue of the fluid continuity equations, $D_{i,j}$, is calculated,

$$D_{i,j} = -(\varepsilon_g \rho_g)_{i,j}^{n+1} + (\varepsilon_g \rho_g)_{i,j}^{n} - \frac{\delta t}{\delta r_i}\left\langle (\varepsilon_g \rho_g) u_g \right\rangle_{i,j}^{n+1} - \frac{\delta t}{\delta z_j}\left\langle (\varepsilon_g \rho_g) v_g \right\rangle_{i,j}^{n+1} + \delta t (\dot{m}_g)_g^n$$

Ideally, for a converged solution, $D_{i,j}$ should be zero. In the code, $D_{i,j}$ is compared with a very small number. The value of the convergence criterion is,

$$D_{i,j} \le CONV_{i,j}^{n+1} = EPSG \cdot (\varepsilon_g \rho_g)_{i,j}^{n}$$

where EPSG is read in. The default and recommended value of EPSG is 10^{-5}.

The computations begin at the left-bottom corner fluid cell. The pressure is corrected in one cell at a time until convergence is obtained or the number of iterations exceed an inner iteration limit. The computations proceed from left to right and from bottom to top until the entire computational regime is covered. At the end of such a computational sweep, if a pressure adjustment was necessary in any of the cells, the procedure is repeated until simultaneous convergence in all the cells is obtained. The number of iterations, however, is restricted by an outer iteration limit.

A.7.3 Pressure Iteration. When $D_{i,j}$ fails to meet the convergence criterion in any cell, the pressure is adjusted using a combination of Newton's method and secant method. The initial adjustment of pressure uses Newton's method.

$$(P_g)^{m+1}=(P_g)^m-\omega\frac{D^m}{\partial D/\partial(P_g)^m}$$

where the indices i, j, and n have been omitted. The index, m, indicates the iteration level. This is equivalent to using Newton's method for each cell, where ω is a relaxation parameter near unity, and $\overline{\beta}$ is computed as,

$$\frac{1}{\overline{\beta}_{i,j}}=\frac{\partial D_{i,j}}{\partial(P_g)_{i,j}}=\frac{\varepsilon_g}{C^2_{i,j}}+(\frac{\delta t}{\delta r_i})^2\left((\varepsilon_g)_{i+\frac{1}{2},j}+(\varepsilon_g)_{i-\frac{1}{2},j}\right)+(\frac{\delta t}{\delta z_j})^2\left((\varepsilon_g)_{i,j+\frac{1}{2}}+(\varepsilon_g)_{i,j-\frac{1}{2}}\right)$$

once every time step. The sound speed $C_{i,j}$ is given by,

$$C^2_{i,j}=\left(\frac{\partial P_g}{\partial \rho_g}\right)_{i,j}$$

where $(\partial P_g/\partial \rho_g)$ can be determined from the equation of state.

This formulation is only approximate. Hence, subsequent corrections use the secant method:

$$(P_g)^{m+1}=(P_g)^m-\omega\left(\frac{(P_g)^{m-1}-(P_g)^m}{D^{m-1}-D^m}\right)D^m$$

The use of secant method is continued until $D_{i,j}$ changes sign. Thereafter a combination of the secant method and a bisection method is used. The method is illustrated in the Figure A.4.

Given the three pressures P_1, P_2, and P_3 of which P_1 and P_2 bracket the desired pressure and P_3 lies between them and the respective mass residuals D_1, D_2, and D_3, do not satisfy the convergence criterion in cell $D_1 > 0$, and $D2 < 0$. With three pressures and their mass residuals obtained as described, or otherwise a constrained two-sided secant technique is used to obtain further pressure adjustments. From these pressures and their

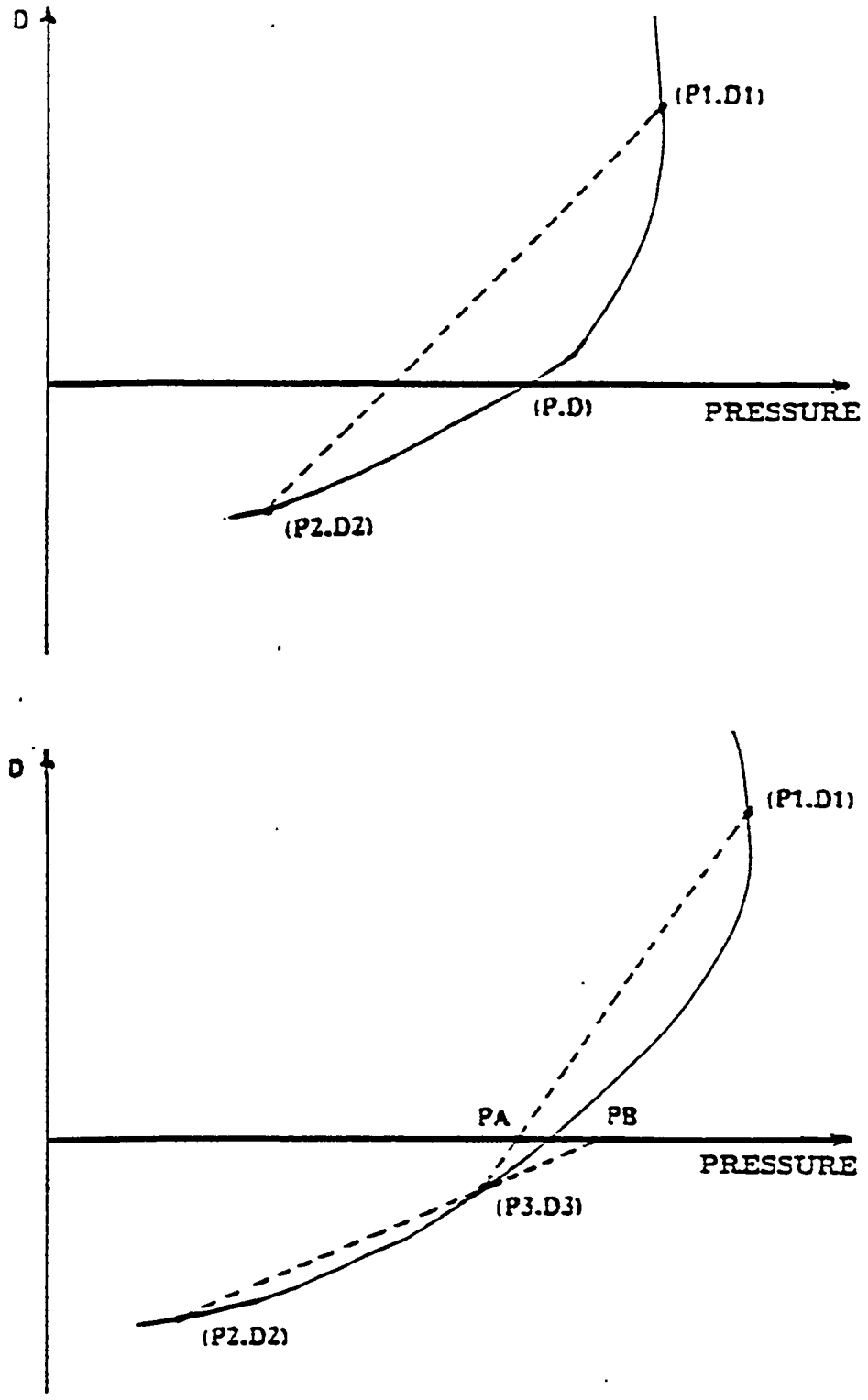

Figure A.4 The Secant method for Pressure Iteration

mass residuals, the pressure P_A and P_B are determined by straight line extrapolation and interpolation, respectively, as follows,

$$p_A=\begin{cases}(p_3D_1-p_1D_3)/(D_1-D_3) & \text{for } D_1\neq D_3\\ (p_2+p_3)/2 & \text{for } D_1=D_3\end{cases}$$

$$p_B=\begin{cases}(p_3D_2-p_2D_3)/(D_2-D_3) & \text{for } D_2\neq D_3\\ (p_1+p_3)/2 & \text{for } D_2=D_3\end{cases}$$

The new estimate of the advanced time pressure is then computed as,

$$(P_g)^{m+1}=\frac{1}{2}(p_A+p_B)$$

If the pressure, P_A should lie outside the interval P_1 to P_3, it is given the value $(P_A+P_B)/2$. After $(Pg)^{m+1}$ is estimated, point 2 is discarded and points 1 and 3 are retained as improved bounds for the next pressure estimate. When $D_{i,j}$ changes sign, the value of $\overline{\beta}_{i,j}$ is also updated for future iterations as,

$$\overline{\beta}=\frac{p_1-p_2}{D_1-D_2}$$

A.7.4 Solution of the Energy Equations. The specific enthalpies $\overline{H}_k$ are calculated in subroutine IGIL accounting for the mass, momentum and energy exchange rates. For the iterative part of the solution, a simplified set of energy equations is used, which is differenced as follows,

$$(\varepsilon_g\rho_g)^{n+1}_{i,j}(\overline{H}_g)_{i,j}=(\varepsilon_g\rho_g)^{n+1}_{i,j}(H_g)^n_{i,j}+\frac{\delta t}{2}\sum_{k=1}^{N}(h_{vk})^n_{i,j}(\overline{T}_k-\overline{T}_g)$$
$$+\delta t\sum_{k=1}^{N}(\beta_{kg})^n_{i,j}\left\{\left((u_k)^n_{i,j}-(u_g)^n_{i,j}\right)^2+\left((v_k)^n_{i,j}-(v_g)^n_{i,j}\right)^2\right\}+(\dot{Q}_{rg}+\dot{Q}_{fg})^n_{i,j}$$

$$(\varepsilon_k\rho_k)^{n+1}_{i,j}(\overline{H}_k)_{i,j}=(\varepsilon_k\rho_k)^{n+1}_{i,j}(H_k)^n_{i,j}+\frac{\delta t}{2}(h_{vk})^n_{i,j}(\overline{T}_g-\overline{T}_k)+(\dot{Q}_{rk}+\dot{Q}_{fk})^n_{i,j}$$

Note that only half the effect of the interface heat transfer is considered here. Thus $\overline{H}$ is some intermediate value between H^n and H^{n+1} defined as,

$$\overline{H}_k = H_k^n + (\overline{T}_k - T_k^n)C_k$$

where, C_k is the specific heat of the fluid or the particulate phases. Rearranging, we get,

$$\overline{T}_k = \frac{\overline{H}_k - H_k^n}{C_k} + T_k^n$$

Thus we get,

$$(\varepsilon_g\rho_g)_{i,j}^{n+1}(\overline{H}_g)_{i,j} = (\varepsilon_g\rho_g)_{i,j}^{n+1}(H_g)_{i,j}^n + (\dot{Q}_{rg} + \dot{Q}_{fg})_{i,j}^n +$$
$$\frac{\delta t}{2}\sum_{k=1}^{N}(h_{vk})_{i,j}^n\left(\frac{(\overline{H}_k)_{i,j} - (H_k)_{i,j}^n}{C_k} + (T_k)_{i,j}^n - \frac{(\overline{H}_g)_{i,j} - (H_g)_{i,j}^n}{C_g} - (T_g)_{i,j}^n\right)$$
$$+\delta t\sum_{k=1}^{N}(\beta_{kg})_{i,j}^n\left\{\left((u_k)_{i,j}^n - (u_g)_{i,j}^n\right)^2 + \left((v_k)_{i,j}^n - (v_g)_{i,j}^n\right)^2\right\}$$

$$(\varepsilon_k\rho_k)_{i,j}^{n+1}(\overline{H}_k)_{i,j} = (\varepsilon_k\rho_k)_{i,j}^{n+1}(H_k)_{i,j}^n + (\dot{Q}_{rk} + \dot{Q}_{fk})_{i,j}^n$$
$$+\frac{\delta t}{2}(h_{vk})_{i,j}^n\left(\frac{(\overline{H}_g)_{i,j} - (H_g)_{i,j}^n}{C_g} + (T_g)_{i,j}^n - \frac{(\overline{H}_k)_{i,j} - (H_k)_{i,j}^n}{C_k} - (T_k)_{i,j}^n\right)$$

In matrix form, $(A_h)_{i,j}(\overline{H})_{i,j} = (B_h)_{i,j}$

Note that $(\varepsilon_k\rho_k)$, $k=g,\ell,s$ are evaluated at time (n+1) and H_k, T_k, h_{vk} are evaluated at time n.

$$(A_h)_{i,j} = \begin{pmatrix} \varepsilon_g\rho_g + \frac{\delta t}{2C_g}\sum_{k=1}^{N}h_{vk} & \frac{\delta t}{2C_1}h_{v1} & \frac{\delta t}{2C_2}h_{v2} & \cdots & \frac{\delta t}{2C_N}h_{vN} \\ \frac{\delta t}{2C_g}h_{v1} & \varepsilon_1\rho_1 + \frac{\delta t}{2C_1}h_{v1} & 0 & \cdots & 0 \\ \frac{\delta t}{2C_g}h_{v2} & 0 & \varepsilon_2\rho_2 + \frac{\delta t}{2C_2}h_{v2} & \cdots & 0 \\ \vdots & \vdots & \vdots & \ddots & \vdots \\ \frac{\delta t}{2C_g}h_{vN} & 0 & 0 & \cdots & \varepsilon_N\rho_N + \frac{\delta t}{2C_N}h_{vN} \end{pmatrix}_{i,j}$$

$$(\overline{\mathbf{H}})_{i,j}=\begin{pmatrix}\overline{H}_g\\ \overline{H}_1\\ \overline{H}_2\\ \vdots\\ \overline{H}_N\end{pmatrix}_{i,j}$$

$$(B_h)_{i,j}=\begin{pmatrix}(\varepsilon_g\rho_g)H_g+(\dot{Q}_{rg}+\dot{Q}_{fg})+\frac{\delta t}{2}\sum_{k=1}^{N}\left\{\begin{matrix}h_{vk}\left(\frac{H_g}{C_g}-\frac{H_k}{C_k}+T_k-T_g\right)\\ +\beta_{kg}\left((u_k-u_g)^2+(v_k-v_g)^2\right)\end{matrix}\right\}\\ (\varepsilon_1\rho_1)H_1+\frac{\delta t}{2}h_{v1}\left(\frac{H_1}{C_1}-\frac{H_g}{C_g}+T_g-T_1\right)\\ (\varepsilon_2\rho_2)H_2+\frac{\delta t}{2}h_{v2}\left(\frac{H_2}{C_2}-\frac{H_g}{C_g}+T_g-T_2\right)\\ \vdots\\ (\varepsilon_N\rho_N)H_N+\frac{\delta t}{2}h_{vN}\left(\frac{H_N}{C_N}-\frac{H_g}{C_g}+T_g-T_N\right)\end{pmatrix}_{i,j}$$

After the converged solution is obtained for the continuity and momentum equations, the solution of the energy equations is completed. The part of the energy equation solved during the iterative solution of the momentum and continuity equations is subtracted from the complete energy equations. Assuming that

$$(\overline{T}_g-\overline{T}_k)\approx(T_g-T_k)^{n+1}$$

we get,

$$T_k^{n+1}=\frac{H_k^{n+1}-\overline{H}_k}{C_k}+\overline{T}_k$$

$$(\varepsilon_g\rho_g)_{i,j}^{n+1}(H_g)_{i,j}=(\varepsilon_g\rho_g)_{i,j}^{n+1}\left((\overline{H}_g)_{i,j}-(H_g)_{i,j}^{n}\right)+(\varepsilon_g\rho_g)_{i,j}^{n}(H_g)_{i,j}^{n}+(\overline{\varepsilon_g\rho_g H_g})_{i,j}$$
$$+\frac{\delta t}{2}\sum_{k=1}^{N}(h_{vk})_{i,j}^{n}\left(\frac{(H_k)_{i,j}^{n+1}-(\overline{H}_k)_{i,j}}{C_k}+(\overline{T}_k)_{i,j}-\frac{(H_g)_{i,j}^{n+1}-(\overline{H}_g)_{i,j}}{C_g}-(\overline{T}_g)_{i,j}\right)+(\dot{Q}_{rg}+\dot{Q}_{fg})_{i,j}^{n}$$

$$(\varepsilon_k\rho_k)_{i,j}^{n+1}(H_k)_{i,j}^{n+1}=(\varepsilon_k\rho_k)_{i,j}^{n+1}\left((\overline{H}_k)_{i,j}-(H_k)_{i,j}^{n}\right)+(\varepsilon_k\rho_k)_{i,j}^{n}(H_k)_{i,j}^{n}+(\overline{\varepsilon_k\rho_k H_k})_{i,j}$$
$$+\frac{\delta t}{2}(h_{vk})_{i,j}^{n}\left(\frac{(H_g)_{i,j}^{n+1}-(\overline{H}_g)_{i,j}}{C_g}+(\overline{T}_g)_{i,j}-\frac{(H_k)_{i,j}^{n+1}-(\overline{H}_k)_{i,j}}{C_k}-(\overline{T}_k)_{i,j}\right)+(\dot{Q}_{rk}+\dot{Q}_{fk})_{i,j}^{n}$$

Solution procedure is same as the one discussed above.

A.8 Boundary Conditions

The rectangular region in which calculations are to performed is partitioned into cells of sizes dx_i (or dr_i) in x (or r)-direction and dy_j (or dz_j) in y (or z)-direction. A perimeter of fictitious (dummy) boundary cells surrounding the computing mesh is used to enforce boundary conditions. Several boundary conditions around the computing mesh perimeter are programmed in the code. The cell flag types are indicated by IFL(I, J).

Flag	Cell Type
1	Fluid cell
2	No-slip rigid walls
3	Free-slip rigid walls for gas/liquid phases, and Partial-slip rigid walls for solid phases
4	Continuous outflow,
5	Prescribed inflow rate,
6	Prescribed pressure inflow,
7	Prescribed pressure outflow with particulate outflow,
8	Prescribed pressure outflow with no particulate outflow,

In the bottom row and left column of boundary cells, any number of inflow openings can be specified using flag types 5 and 6. Similarly, in the top row and right column of boundary cells, any number of outflow openings can be specified using flag

types 4, 7 and 8. Flag types 2 and 3 may be prescribed on any of the four boundaries to represent rigid (solid) cells. Obstacles blocks within the computing mesh are built from rigid cells, flag types (IFL = 2 or 3).

The position of all blocks must coincide with rectangular cells within the computing mesh. Calculations are not performed in the obstacle cells, only in the remaining fluid cells within the computing mesh. Cell flag type (IFL =1) is a computational cell.

A.8.1 Rigid Cells. Three types of boundary conditions may be specified for a rigid (solid) cell: free-slip, no-slip or partial slip (IFL = 2 or 3). In two dimensions, a free-slip boundary represents line of symmetry and a non-adhering boundary that exerts no drag on the fluid; a no-slip boundary represents a viscous boundary that exerts a drag on the fluid.

Consider cell (i, j), which is a fluid cell, an inflow boundary cell, or an outflow boundary cell. An adiabatic rigid cell is said to be a corner cell if and only if it has at least two adjacent edges, each of which is shared with a fluid cell, an inflow boundary cell, or an outflow boundary cell.

If right cell (i+1, j) or left cell (i-1, j), is a rigid cell, then for all time levels n

$$(u_k)^{n+1}_{i\pm\frac{1}{2},j} = 0$$

$$(v_k)^{n+1}_{i\pm1,j+\frac{1}{2}} = \begin{cases} (v_k)^{n}_{i,j+\frac{1}{2}} & \text{for} \quad \text{IFL=2} \\ -(v_k)^{n}_{i,j+\frac{1}{2}} & \text{for} \quad \text{IFL=3} \end{cases}$$

Similarly, if top cell (i, j+1) or bottom cell (i, j-1), is a rigid cell and if free-slip boundary conditions (IFL = 2) or no-slip boundary conditions (IFL = 3) are imposed, then for all n,

$$(u_k)^{n+1}_{i+\frac{1}{2},j\pm1} = \begin{cases} (u_k)^n_{i+\frac{1}{2},j} & \text{for} \quad \text{IFL=2} \\ -(u_k)^n_{i+\frac{1}{2},j} & \text{for} \quad \text{IFL=3} \end{cases}$$

$$(v_k)^{n+1}_{i,j\pm\frac{1}{2}} = 0$$

If any one of the cells (i, j+1), (i+1, j), (i-1, j), or (i, j-1) is both a rigid cell and a corner cell, then, for all free-slip, no-slip and partial-slip boundary conditions, all its velocity components located at the center are set equal to zero.

A.8.2 Inflow Boundary Cells. For each inflow opening a pressure, P_g, velocities u_k and v_k, and volume fractions, ε_k for all phases ($k=g,\ell,s$), temperature of all phases T_k ($k=g,\ell,s$), composition, y_k^j ($k=g,\ell,s$), and solids granular temperature Θ_k must be specified in the input data, as necessary.

The types of inflow boundary conditions used are inflow prescribed (IFL 5); or inflow pressure prescribed, (IFL = 6). The pressure, P_g, is required for -both (IFL = 5) and (IFL = 6) to compute the mass fluxes. However, when the inflow pressure is prescribed, the radial or axial velocity components are computed using momentum equations.

A.8.3 Outflow Boundary Cells. For each outflow opening, a pressure, P_g may be specified at the beginning of each computation cycle. For constant boundary conditions, the value of P_g is that specified in the input data. The types of outflow boundary conditions used are: pressure prescribed outflow with particulate outflow (IFL=7), or no particulate outflow (IFL = 8); or continuous outflow (IFL = 4).

For both pressure-specified and continuous outflow boundary conditions, the volume fractions, for a given cell of an outflow opening, is obtained by reflection. The

tangential components of the velocities are set to zero. A numerical screen is used to keep particulate phases from leaving the fluidized bed for (IFL = 8).

Therefore, at the top outflow boundary, where (i,j)=(I, JB2); (i+1/2, j)=(I, JB2); (i, j+1/2)=(I, JB2); (i, j-1)=(I, JB2); and (i, j-1/2)=(I, JB1), we have,

$$(P_g)_{i,j}^{n+1}=\begin{cases}P_0 & \text{for} \quad \text{IFL=7/8}\\ (P_g)_{i,j-1}^{n} & \text{for} \quad \text{IFL=4}\end{cases}$$

$$(\varepsilon_k)_{i,j}^{n+1}=\begin{cases}(\varepsilon_k)_{i,j-1}^{n} & \text{for} \quad \text{IFL=4/7}\\ 1 \quad k=g & \text{for} \quad \text{IFL=8}\\ 0 \quad k\neq g & \end{cases}$$

$$(u_k)_{i+\frac{1}{2},j}^{n+1}=0$$

$$(v_g)_{i,j+\frac{1}{2}}^{n+1}=(\varepsilon_g\rho_g)_{i,j-1}^{n+1}(v_g)_{i,j-\frac{1}{2}}^{n+1}\Big/(\varepsilon_g\rho_g)_{i,j}^{n+1}$$

$$(v_k)_{i,j+\frac{1}{2}}^{n+1}=\begin{cases}(\varepsilon_k\rho_k)_{i,j-1}^{n+1}(v_k)_{i,j-\frac{1}{2}}^{n+1}\Big/(\varepsilon_k\rho_k)_{i,j}^{n+1} & \text{for} \quad \text{IFL=4/7}\\ 0 & \text{for} \quad \text{IFL=8}\end{cases}$$

At the right outflow boundary, where (i, j)=(IB2, j); (i+1/2, j)=(IB2, J); (i-1, j)=(IB1,J); (i-1/2, j)=(IB1, J); and (i-1, j)=(IB1, J).

$$(P_g)_{i,j}^{n+1}=\begin{cases}P_0 & \text{for} \quad \text{IFL=7/8}\\ (P_g)_{i-1,j}^{n} & \text{for} \quad \text{IFL=4}\end{cases}$$

$$(\varepsilon_k)_{i,j}^{n+1}=\begin{cases}(\varepsilon_k)_{i-1,j}^{n} & \text{for} \quad \text{IFL=4/7}\\ 1 \quad k=g & \text{for} \quad \text{IFL=8}\\ 0 \quad k\neq g & \end{cases}$$

$$(u_g)_{i+\frac{1}{2},j}^{n+1}=(\varepsilon_g\rho_g)_{i-1,j}^{n+1}(u_g)_{i-\frac{1}{2},j}^{n+1}\Big/(\varepsilon_g\rho_g)_{i,j}^{n+1}$$

$$(u_k)_{i+\frac{1}{2},j}^{n+1}=\begin{cases}(\varepsilon_k\rho_k)_{i-1,j}^{n+1}(u_k)_{i-\frac{1}{2},j}^{n+1}\Big/(\varepsilon_k\rho_k)_{i,j}^{n+1} & \text{for} \quad \text{IFL=4/7}\\ 0 & \text{for} \quad \text{IFL=8}\end{cases}$$

$$(v_k)^{n+1}_{i,j+\frac{1}{2}}=0$$

A.9 Initial Conditions

At the beginning of the simulation the distribution of all field variables is given by the initial conditions. Uniform and simple non-uniform initial conditions can be specified using the input data. Fluid blocks IFL = 1) with the field variables may be defined in similar manner as the obstacle blocks are defined. Complex non-uniform initial conditions should be programmed.

The pressure in the axial direction is initialized by the gravity head of the fluid or/and particulate phases. If (IPRES = 0), pressure profile is obtained using fluid phase only and the weight of the particulate phases is not supported by fluid phase. If (IPRES = 1), the fluid phase supports the weight of the complete bed.

The pressure distribution in all fluid cells is computed recursively from the weight of the bed as follows,

$$(P_g)_{i,j}=(P_g)_{i+1,j}-g_z\delta z_{j+\frac{1}{2}}\begin{cases}(\varepsilon_g\rho_g)_{i,j+\frac{1}{2}} & \text{for} \quad \text{IPRES=0}\\ \sum_{k=g,1}^{N}(\varepsilon_k\rho_k)_{i,j+\frac{1}{2}} & \text{for} \quad \text{IPRES=1}\end{cases}$$

where pressure in the top most cell J = JB2 is given by $(P_g)_{i,j+1/2}=P_0$. For density of fluid, equation of state may be used. Since this density may depend on the pressure in cell (i, j) which is yet to be calculated, a quadratic equation must be solved in a general case.

In a rigorous approach, the pressure distribution in a two-dimensional region must be computed by solving the finite differenced continuity and momentum equations with initial values of volume fractions, velocities and temperatures of all required phases.